

# **GEOSTATISTICAL ANALYSIS OF PRODUCTION TRENDS IN THE PERMIAN BASIN**

---

**LISA M. ZOELICK, MGIS CANDIDATE**

**APRIL 16, 2016**

# TABLE OF CONTENTS

<b>ABSTRACT .....</b>	<b>3</b>
<b>I. INTRODUCTION.....</b>	<b>4</b>
<b>II. BACKGROUND .....</b>	<b>4</b>
II.1    GEOGRAPHY.....	4
II.2    GEOLOGY .....	4
II.3    PETROLEUM INDUSTRY.....	5
<b>III. CHALLENGES.....</b>	<b>6</b>
III.1    FORMATION CLASSIFICATION.....	6
III.2    PRODUCTION VISUALIZATION.....	6
<b>IV. OBJECTIVES .....</b>	<b>7</b>
<b>V. METHODOLOGY.....</b>	<b>7</b>
V.1    OBTAINING DATA .....	7
V.2    EXPLORATORY SPATIAL DATA ANALYSIS.....	8
V.3    KRIGING.....	10
<i>V.3.1 Benefits of Kriging.....</i>	<i>10</i>
<i>V.3.2 Limitations of Kriging.....</i>	<i>10</i>
V.4    EMPIRICAL BAYESIAN KRIGING .....	11
<i>V.4.1 Applying EBK to the Permian Basin Team's Data .....</i>	<i>12</i>
V.5    CROSS VALIDATION AND VISUALIZATION.....	13
<i>V.5.1 Cross Validation Table and Graphs.....</i>	<i>13</i>
<i>V.5.1 Standard Error Visualization.....</i>	<i>14</i>
<b>VI. RESULTS.....</b>	<b>15</b>
VI.1    CLASSIFYING WELLS BY HORIZONS.....	15
VI.2    INCORPORATING PETROPHYSICS.....	16
VI.3    GENERATING 3D SURFACES .....	17
VI.4    VISUALIZING PRODUCTION .....	18
<b>VII. SUMMARY.....</b>	<b>19</b>
VII.1    INTEGRATED PLATFORM.....	19
<b>ACKNOWLEDGEMENTS.....</b>	<b>23</b>
<b>REFERENCES.....</b>	<b>23</b>

## **ABSTRACT**

Due to data volume and geologic complexity, maps illustrating the distribution of production in the Permian Basin require data integration to understand and display geologic properties and production history. This project demonstrates how production and well properties across an entire basin can be related to specific geologic horizons through quantifying existing data using geographic information systems (GIS).

The Permian Basin contains geologic zones that can be more than 3,000 feet thick, often with multiple productive horizons and specific petrophysical properties. Traditionally, areas have been investigated through time-consuming evaluation of individual well logs. This study used GIS to extend classifications by utilizing interpreted depths and metrics from raw well logs to perform geostatistical interpolation across the basin. This process has reduced evaluation time through streamlined assessment of thousands of wells.

Classification of the producing horizons, in addition to the geologic, petrophysical, and engineering properties have helped identify trends related to petroleum production and increased our understanding of the relationship between variables that allow for a play to be successful.

# I. INTRODUCTION

This report details how geographic information systems (GIS) can be used to model sub-surface parameters to gain a better understanding of basin properties and production trends. This workflow improves the efficiency of basin appraisal through extending geologists' classifications to areas that have not been evaluated.

GIS, with a robust platform designed to incorporate and manage complex datasets, is uniquely equipped to serve as a platform to disseminate information from various disciplines and provide output of the new analyses performed in GIS that can be consumed by software applications in each discipline.

# II. BACKGROUND

## II.1 GEOGRAPHY

The Permian Basin covers a large geographic area made up of 52 counties and more than 75,000 square miles (48 million acres) in western Texas and southeastern New Mexico. The Permian Basin, illustrated in Figure 1, is split into two main sub-basins, the Midland Basin in the east and the Delaware Basin in the west.

## II.2 GEOLOGY

In addition to covering a large geographic area, the Permian Basin is also geologically complex containing 23 prospective formations with up to “25,000 feet of multiple, stacked, petroleum systems” (Matador Resources Company, 2015). The producing formations of the Permian Basin are shown in Figure 2 with a stratigraphic chart representing the producing formations of both basins and the intervening Central Basin Platform.

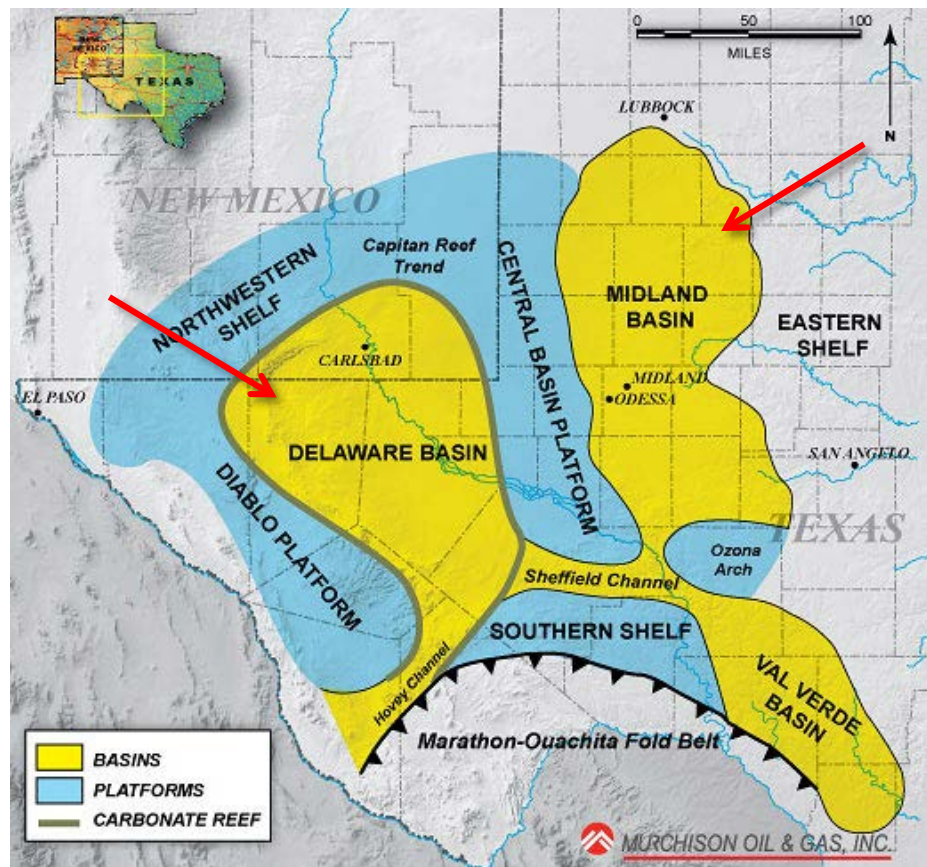


Figure 1: Map of Permian Basin Structural Setting. Murchison Oil and Gas. 2010. Web. 9 Oct 2015.

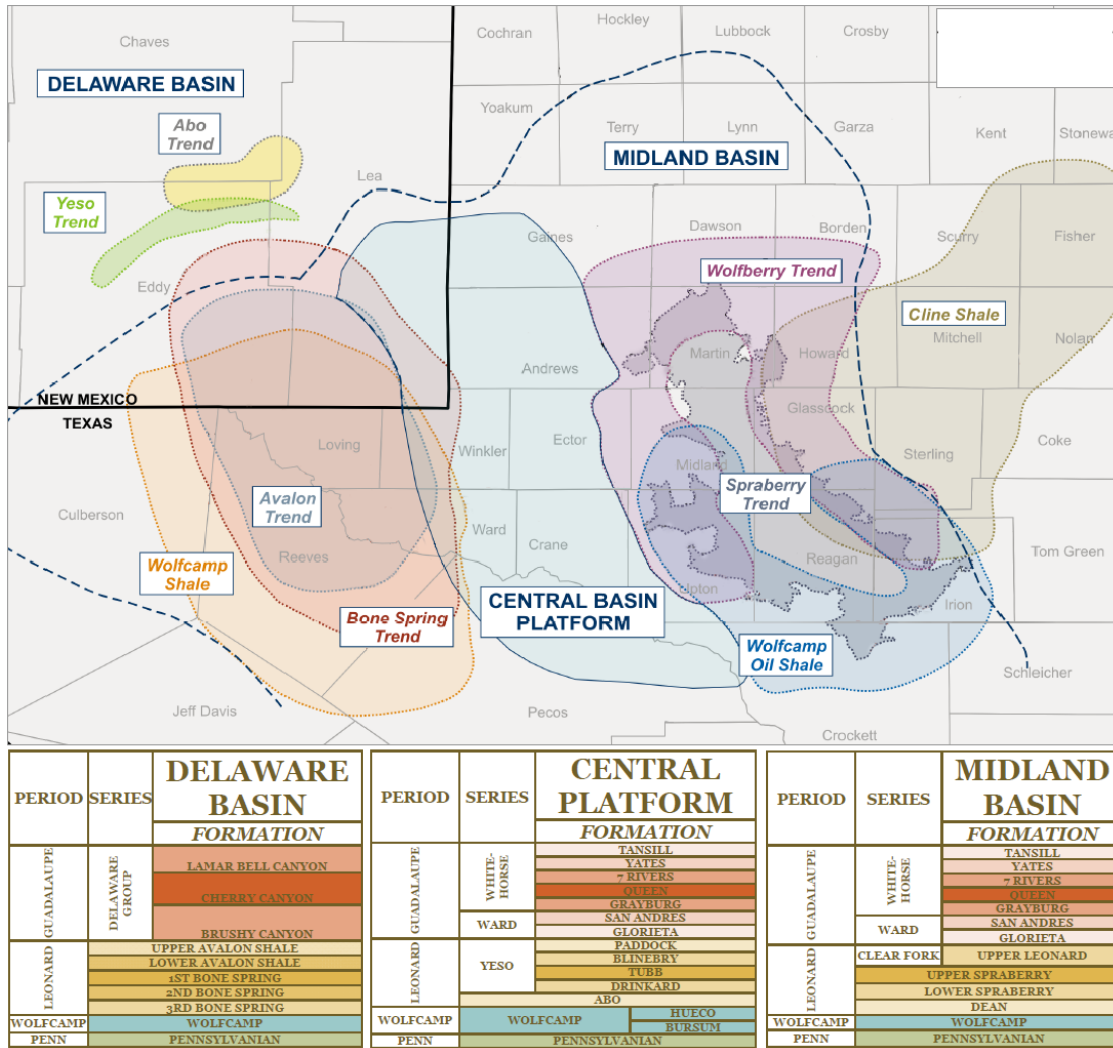


Figure 2: Map of sub-basins and stratigraphy in the Permian. Shale Experts. 2015. Web. 13 Nov 2015.

### II.3 PETROLEUM INDUSTRY

“Extensive drilling, coring, and geological studies have been conducted since the 1920s” (Matador, 2015) with more than 1,000 operators and over 500,000 wells drilled during the past 95 years. The Texas Railroad Commission (the Commission), which regulates the state’s oil and gas activity, notes that in Texas “The Permian Basin has produced over 29 billion barrels of oil and 75 trillion cubic feet of gas and it is estimated by industry experts to contain recoverable oil and natural gas resources exceeding what has been produced over the last 90 years” (Railroad Commission of Texas, 2013).

Throughout 2014 and 2015, about 15,000 wells were drilled in the Permian Basin. Of these, 75% were drilled in 2014. Drilling activity, along with the commodity prices for oil and natural gas, have steadily fallen. However, the production rates across the basin vary widely; all areas are not economically viable. To create value at today’s commodity prices, the best spots in the play must be identified through valuation of producing horizons, and examining the optimum combination of geologic, reservoir, and engineering properties that allow the basin to be productive.

## III. CHALLENGES

### III.1 FORMATION CLASSIFICATION

Although the Commission requires operators to report the producing formation for each well, an individual formation can be more than 3,000 feet thick and contain multiple productive horizons. Since the Commission does not mandate that an operator disclose which horizon or interval within a formation is producing, geologists must determine the producing interval through time-consuming evaluation of individual well log data.

### III.2 PRODUCTION VISUALIZATION

The challenge continues after the producing horizon has been identified. Due to the volume and complexity of data representing multiple stacked geologic horizons, conventional 2D maps showing the production distribution in the Permian Basin are unable to capture the entire story; producing horizons within a formation cannot be inferred. While some areas may look as though they have low production rates, it is possible that untapped formations still have production potential that have not been explored. To make informed decisions, detailed information about what makes the area productive or seemingly unproductive is needed to understand and evaluate the production trend.

Discrepancies in horizon identification as well as inefficiencies in using 2D data have pushed innovative ideas on integrating different disciplines together. Figure 3 is an example of bringing data from different disciplines together in an integrated 3D model to better visualize the impact of the many parameters needed to consider an area's production trends. Here, geologic information is shown by the color of the wellbores; the charts show the general production intervals of oil, gas, and water; and the seismic 3D cross-section and 3D volume are used to evaluate the geophysics.

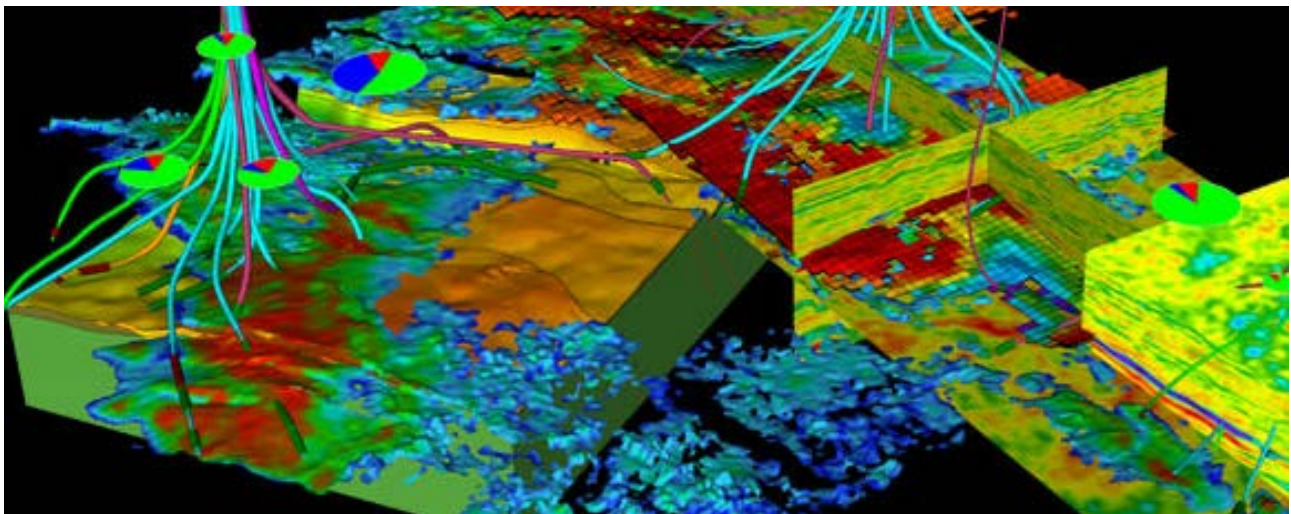


*Figure 3: Integrated 3D model displaying data from different disciplines including well deviation surveys, a seismic cross section and 3D volume, and production information displayed in the pie charts. Dynamic Graphics. 2015. Web. 10 Dec 2015.*

## IV. OBJECTIVES

The Permian Basin team requested a process to streamline basin evaluation. GIS was evaluated as a tool to generate a solution to provide a repeatable workflow which would systematize the evaluation of large quantities of data quickly. This workflow has the potential to extend the geologists' classifications by utilizing interpreted well logs to perform geostatistical interpolation. Interpolation uses point data that contain a value for a specified parameter to create a continuous surface. In this case, the interpolation would sub-delineate, or break down larger units in the formation, into contiguous producing horizons that can be correlated, and will also be used to create continuous surfaces representing an average value for petrophysical properties within the horizon. The process will then classify completion and production from productive zones and provide a robust well dataset that can be used by each discipline.

## V. METHODOLOGY

### V.1 OBTAINING DATA

The first step of the workflow is obtaining data from the geologist. This dataset includes unique identifiers for the evaluated wells, the sub-delineated horizon name, the total vertical depth in subsea (TVDSS) at the surface of the horizon, and petrophysical metrics from evaluated well logs.

Gamma ray, resistivity, neutron porosity, and bulk density were assessed from the well logs. An example of an interpreted well log depicting the geologic benchmarks and individual parameter values is illustrated in Figure 4. Gamma ray, in the first track, is a passive detection of natural gamma radiation that measures the radioactivity of rocks to assist with lithology identification (Asquith and Krygowski, 2004). Everything is naturally radioactive, however shale is more radioactive due to decay of trace elements over geologic time (Boyce, 2015). In the well log example, the light grey and black colors indicate shale, and the yellow indicates sand in the formation.

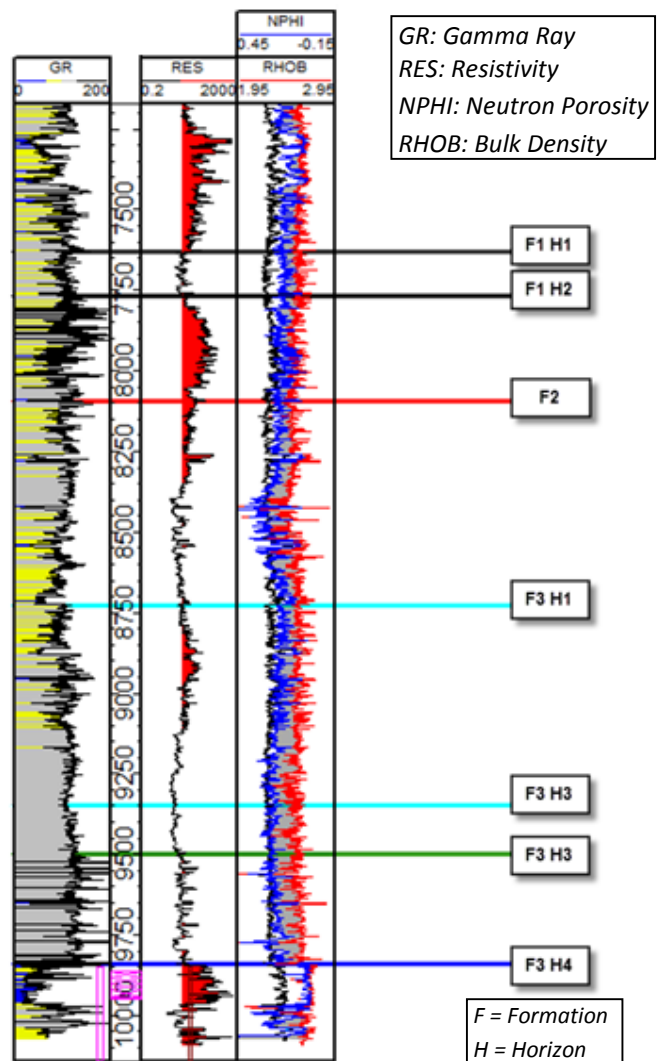


Figure 4: Interpreted well log. Matt Boyce, PhD. 2013. Southwestern Energy. 7 Dec 2015.

Resistivity, in the second track, is used in formation evaluation to determine where hydrocarbon and water zones occur and is used to indicate an estimate of permeability, porosity, and lithology. This is accomplished by measuring the electrical resistivity in the rock's matrix. Since different fluids including salt water, fresh water, oil, and gas have different conductive properties, the log response can be evaluated to determine what type of fluids are in the formation (Asquith and Krygowski, 2004).

Neutron porosity and bulk density, shown in the third track, are used in conjunction to determine lithology, porosity, and potential hydrocarbon zones. Neutron porosity is determined by measuring the hydrogen concentration in the fluids within the pore space in a formation (Asquith and Krygowski, 2004). Bulk density is determined when the emitted gamma rays collide with electrons in the formation (Asquith and Krygowski, 2004).

Once these data are received, they are brought into Esri's ArcGIS software and a point dataset is created from the well coordinates.

## **V.2 EXPLORATORY SPATIAL DATA ANALYSIS**

Before beginning any data interpolation, it is important to perform exploratory data analysis in order to understand the data being modelled and detect any inconsistencies in the dataset (Chiles and Delfiner, 2012). To achieve the most accurate interpolation results, the dataset should have a Gaussian, or normal distribution. ArcGIS provides quantitative data exploration tools in the Exploratory Spatial Data Analysis (ESDA) toolset to assist in discerning the distributions. In addition to quality control checking the data and determining the best methodology to interpolate information, these tools assist with examining the data distribution, identifying local and global outliers, visualizing the overall trends, and examining the spatial autocorrelation across the dataset. "Spatial autocorrelation quantifies the assumption that things that are closer are more alike than things that are farther apart" (Esri, 2015). Using these tools, the datasets were reviewed, quality assurance was performed, and the optimum methodology was chosen to interpolate the data.

The ESDA toolset was used to evaluate the data received from the Permian Basin team. The histogram and the normal quantile-quantile plot (normal q-q plot) shown in Figure 5 were created from the ESDA tools. The histogram is used to "graphically summarize the distribution of a univariate data set" (NIST, 2012). The normal q-q plot is used to visually assess if the data are normally distributed by plotting the quantiles, or percentage of points in the dataset, against a standard normal distribution which is represented as a straight 45° line (NIST, 2012). The closer to the 45° line the points plot, the closer the dataset is to having a normal distribution.

The histogram was divided into a user-defined number of bins or groups that show the frequency of the chosen attribute in the dataset. Although the dataset for each horizon was unique, and the histogram with each varied, the graphs are meant to illustrate a representative sample of the data kriged in this project. In addition to visually assessing the data distribution, the statistics information in the upper right portion of the histogram reveals important information to assist in understanding the data's distribution. Indicators of a normal distribution on the histogram include: a bell-shaped



curve, the mean and median will have close to the same value; the skewness, which measures how symmetrical the data are, should be close to zero; and the kurtosis, which indicates how thick the tails of the histogram are, should be close to three (NIST, 2012).

Both the histogram and the normal q-q plot graphs display the distribution of points containing depth information for one of the geologic horizons. The ESDA tools offer “linked highlighting” which enables the user to interact with the data by selecting individual data points on the normal q-q plot or a bar on the histogram to identify their location and determine how the data are related. This improves quality control by allowing the user to select outliers and examine their assigned value to ensure there are no erroneous data points that could impact the model.

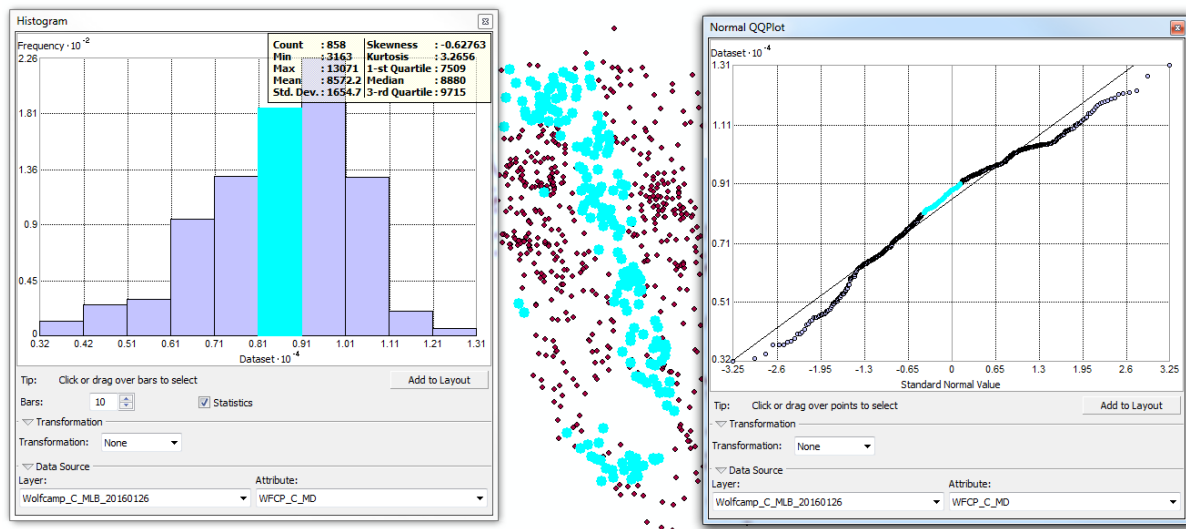


Figure 5: ESDA tools (left, histogram; right, normal QQ plot) exhibit data distribution of depth attribute from interpreted well logs.

Once data quality evaluation was completed, deterministic and probabilistic interpolation methods were evaluated to provide the most reliable results. The software the geologists use applies a deterministic direct linear interpolator to create surfaces. Deterministic methods use defined algorithms that take into account the distance between a known location and a queried location, while probabilistic methods use a statistical approach and “quantify the uncertainty associated with the interpolated values” (Krivoruchko, 2012).

Various interpolation techniques offered in Esri’s ArcMap were evaluated including: natural neighbors, inverse distance weighting (IDW) averaging, and different types of kriging. Traditional deterministic methods of interpolation are widely used because of the low computational cost and ease to run, but these methods have a number of shortcomings (Chen, 2014). One of the most popular deterministic methods of interpolation, IDW, like other predictive interpolators, uses the distance between locations to predict a value, but it is not able to account for the underlying spatial relationship, or the direction of how points are related (Flitter et al., 2013). IDW also produces “boundary bias” which is the “bias of the function estimates is larger at the boundary of the exploratory variable space than in the interior” (Chen, 2014) and also produces a “bull’s eye” effect

creating circular areas around the known values of the data (Achilleos, 2008). After visually inspecting the output of the different interpolations and reviewing them with the Permian Basin team, the team requested a probabilistic method that would allow for visualization of the precision of the interpolation across the predicted surface.

### **V.3 KRIGING**

Kriging utilizes a Gaussian statistical model to optimize spatial prediction and has applicability in diverse fields such as “mining, petroleum engineering, meteorology, soil science, precision agriculture, pollution control, public health, monitoring fish stocks and other animal densities, remote sensing, ecology, geology, hydrology and other disciplines” (Fischer and Getis, 2010).

Danie Gerhardus Krige, a South African mining engineer, pioneered kriging in the early 1950’s for use with mineral resources management. Georges Matheron, a French mathematician who coined the term “kriging” and founded mathematical morphology, formalized Krige’s work in the 1960’s supplying the “theoretical framework of geostatistics” (Fischer and Getis, 2010). In addition to Krige and Matheron, a number of individuals from different disciplines also developed geostatistical methodologies that can be traced back to “Mercer and Hall (1911), Youden and Mehlich (1937), Kolmogorov (1941), Gandin (1965), and Matérn (1960)” (Fischer and Getis, 2010).

#### ***V.3.1 Benefits of Kriging***

Kriging has a number of benefits. “Most mathematical methods take account of systematic or deterministic variation only and disregard the errors of prediction. Kriging, on the other hand... makes the best use of existing knowledge by taking account of the way a property varies in space through the variogram or covariance function” (Fischer and Getis, 2010).

Another attribute that sets kriging apart from other interpolators is that it accounts for both the distance and the direction of the data. “Kriging is a method of optimal prediction or estimation in geographical space, often known as a best linear unbiased predictor (BLUP). It is the geostatistical method of interpolation for random spatial processes” (Fischer and Getis, 2010). Generally speaking, kriging predictors have smaller uncertainty than other prediction models and have the ability to filter out measurement errors (Krivoruchko, 2012).

Kriging also uses a semivariogram, which is a function of the distance and direction separating two locations, to quantify the spatial dependence in the data. “Accurate variogram estimation is crucial for making reliable predictions on the basis of spatially correlated data (Castruccio, 2012). Kriging offers other advantages including robust cross-validation and the ability to generate prediction, quantile, and standard error maps which quantify the amount of uncertainty associated with the interpolation across the surface.

#### ***V.3.2 Limitations of Kriging***

Kriging assumes the semivariogram it develops is always correct when applying its function to the data. Kriging is an optimal interpolator when the data distribution follows a Gaussian distribution (Pardo- Igúzquiza and Dowd, 2015). However, in cases where the data distribution is not Gaussian,

the error is underestimated (Pilz and Spöck, 2007). To create an accurate model, the semivariogram must create an accurate algorithm of the data. Optimal models achieve maximum efficiency when the data conform to the model, but can lead to poor results when the data does not follow the model; robust models are able to account for the variations in the data distribution without negatively impacting the overall results (Chiles and Delfiner, 2012). Since real world data is unlikely to follow an exact distribution, a robust methodology that offers the advantages of kriging was evaluated to interpolate the data. “The first steps towards Bayesian prediction in spatial linear models were made by Kitanidis (1986), Omre (1987) and Omre and Halvorsen (1989)” (Pilz and Spöck, 2007). Chiles and Delfiner (2012) note that “in petroleum reservoir evaluation... Bayesian approaches are well-suited for reservoir characterization.”

#### V.4 EMPIRICAL BAYESIAN KRIGING

Empirical Bayesian Kriging (EBK) attempts to account for the uncertainty introduced in the semivariogram in ordinary kriging (Esri, 2015). To achieve this, the EBK tool creates subsets in the dataset and simulates a semivariogram for each data subset. This allows the tool to account for local and global variation in the data and create a unique function to fit the semivariogram for each data subset. EBK can also provide relatively accurate predictions of non-stationary data and achieves better accuracy than other kriging for small datasets (Esri, 2015).

Using the iterations of the semivariogram, the EBK model is able to remove the local trend in the dataset. In cases where the data is not normally distributed, a transformation can be applied to the dataset to obtain the most accurate results as demonstrated by Krivoruchko (2012) in Figure 6. Figure 6A illustrates a dataset that has a positively skewed distribution. Figure 6B depicts a transformation function applied to the skewed dataset. The results of the applied transformation are a Gaussian distribution that will be more precisely modeled as illustrated in Figure 6C.

The geostatistical analyst (GA) “wizard” in ArcMap provides a user interface where parameters were chosen to create the following: subsets in the data, an overlap factor, the number of simulations, sector type, and a minimum and maximum number of neighbors to consider when creating the surface. “Unlike other kriging methods (which use weighted least squares), the semivariogram parameters in EBK are estimated using restricted maximum likelihood (REML)” (Esri, 2015). The default parameter for the number of simulations is 100, meaning that the model would

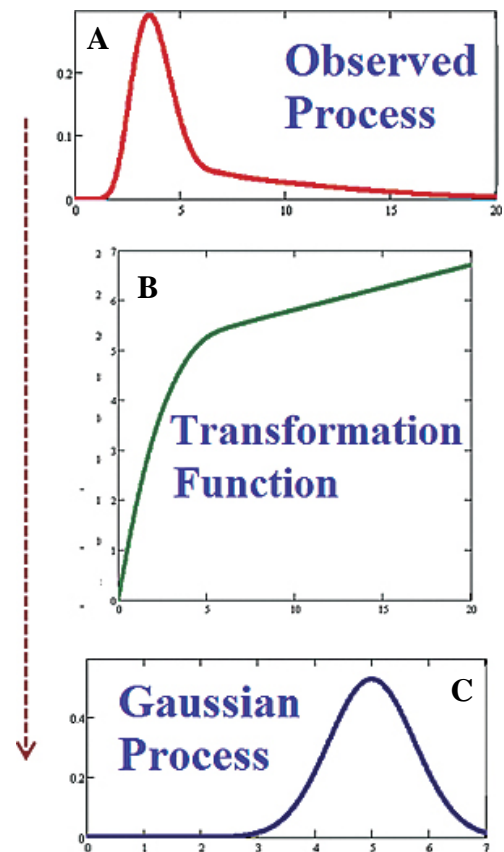


Figure 6: Applying a transformation to an observed process. “Empirical Bayesian Kriging.” Krivoruchko, 2012.

be run 100 times, creating a semivariogram each time. This information is used to quantify the probability of a specific simulation occurring. Esri affirms that unlike other kriging models that assume a trend applies to the whole dataset, EBK uses “intrinsic random functions that inherently correct for trends in the data” (Esri, 2015). EBK was chosen as the interpolation tool to analyze the data supplied by the Permian Basin team.

#### V.4.1 Applying EBK to the Permian Basin Team’s Data

EBK “creates a large number of semivariograms for each subset, and when they are plotted together, the result is a distribution of semivariograms that are shaded by density (the darker the blue color, the more semivariograms pass through that region)” (Esri, 2015). Figure 7 illustrates samples of the EBK distribution of semivariograms generated from the dataset provided by the Permian Basin team for two unique values within the same dataset. The x-axis shows the distance between the predicted value and the neighboring value used to create the semivariogram and the y-axis shows the number of simulations. The semivariogram distribution can be viewed for each point in the dataset. The empirical semivariances are signified with the blue crosses, the median distribution is indicated with a solid red line and the 25<sup>th</sup> and 75<sup>th</sup> percentiles are shown with dashed red lines (Esri, 2015). There are many semivariogram models to choose from (depending on if a transformation is used in the data) including: power, linear, thin plate spline, exponential, whittle, and K-Bessel. The different models each have specific advantages and disadvantages including flexibility, accuracy, and calculation time.

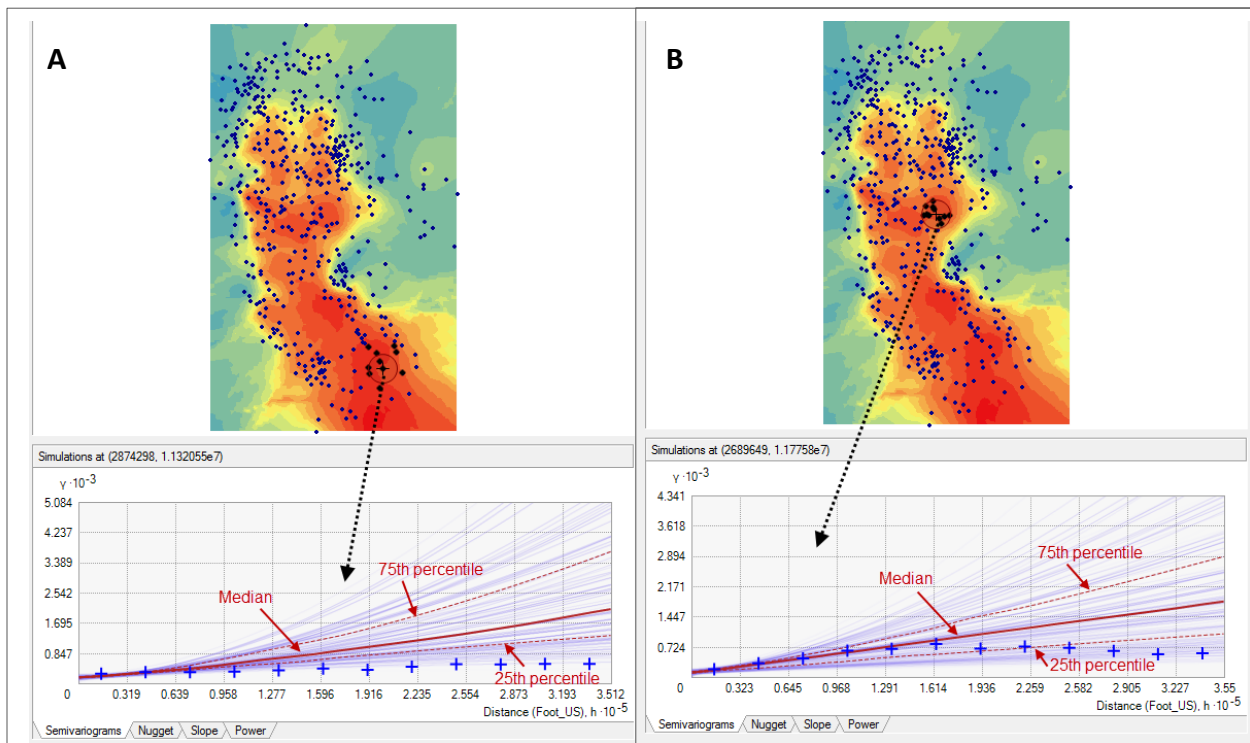


Figure 7: Illustration of distribution of semivariograms with 100 iterations for two unique locations in dataset.

## V.5 CROSS VALIDATION AND VISUALIZATION

### V.5.1 Cross Validation Table and Graphs

Another powerful advantage of using kriging to model the data is that it provides cross validation. “The principle of cross-validation, also called “leave-one-out method,” is to estimate  $Z(x)$  at each sample point  $x\alpha$  from neighboring data  $Z(x\beta)$ ,  $\beta \neq \alpha$ , as if  $Z(x\alpha)$  were unknown. Thus at every sample point  $x\alpha$  we get a kriging estimate  $Z^*_\alpha$  and the associated kriging variance  $\sigma^2/K\alpha$ ” (Chiles and Delfiner, 2012). In other words, cross-validation is achieved as follows: each point in the dataset is removed systematically, one at a time while the rest of the dataset is used to predict the value of the location that was removed. The predicted value and actual value for the point are then compared to determine the measurement error of the prediction. The cross-validation table in Figure 8 shows the result of the tool removing individual points and determining the error associated with a given location. The predicted points, errors, and standard errors are graphed as can be seen in Figure 8. Similar to the ESDA tools, the cross-validation graphs allow the user to interactively select points and see them highlighted in the cross-validation table and on the map. The standard error and standardized errors are generally smaller than traditional kriging methods which can be traced back to the data being modelled with many semivariograms (Krivoruchko, 2012).

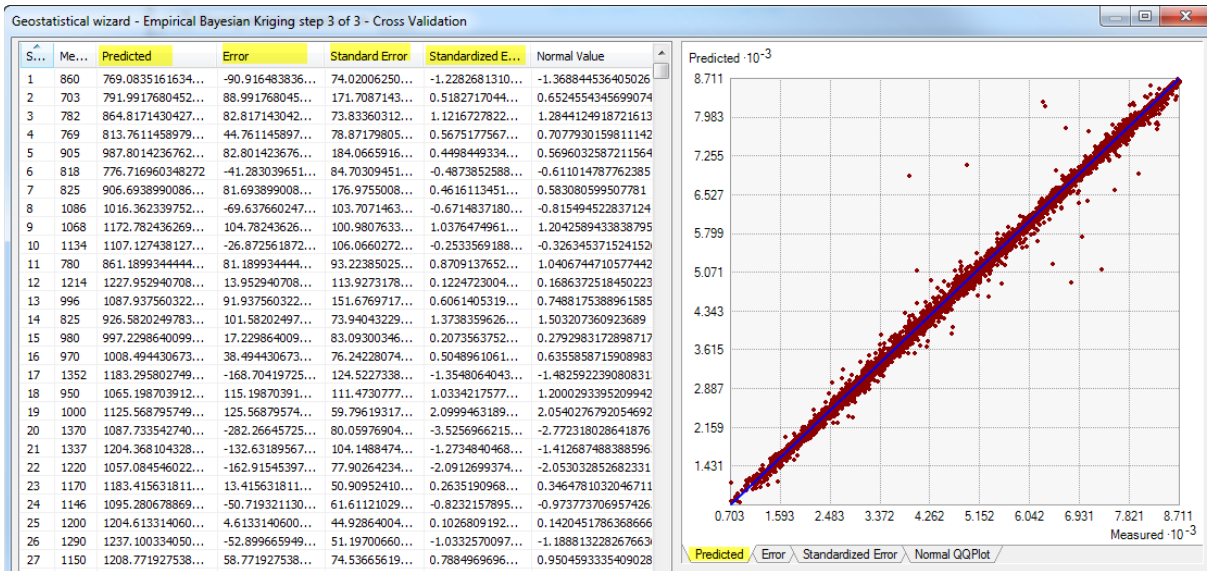


Figure 8: Cross validation chart and predicted values graph.

Figure 9 shows a summary of the cross validation table depicting statistics for the entire dataset instead of individual points. Ideally, the mean standardized error (MSE) should be close to zero, the root-mean-square (RMS) standardized error should be near one, and the average standard error (ASE) should be as small as possible. A large RMS standardized error indicates an unstable model. When adjusting the

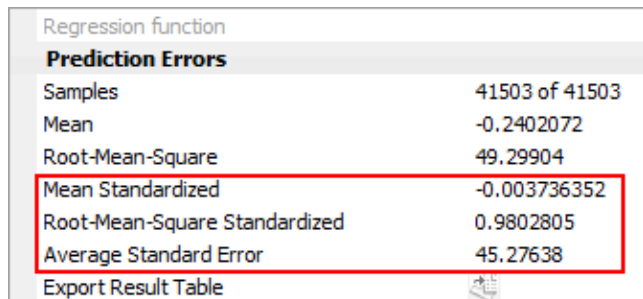
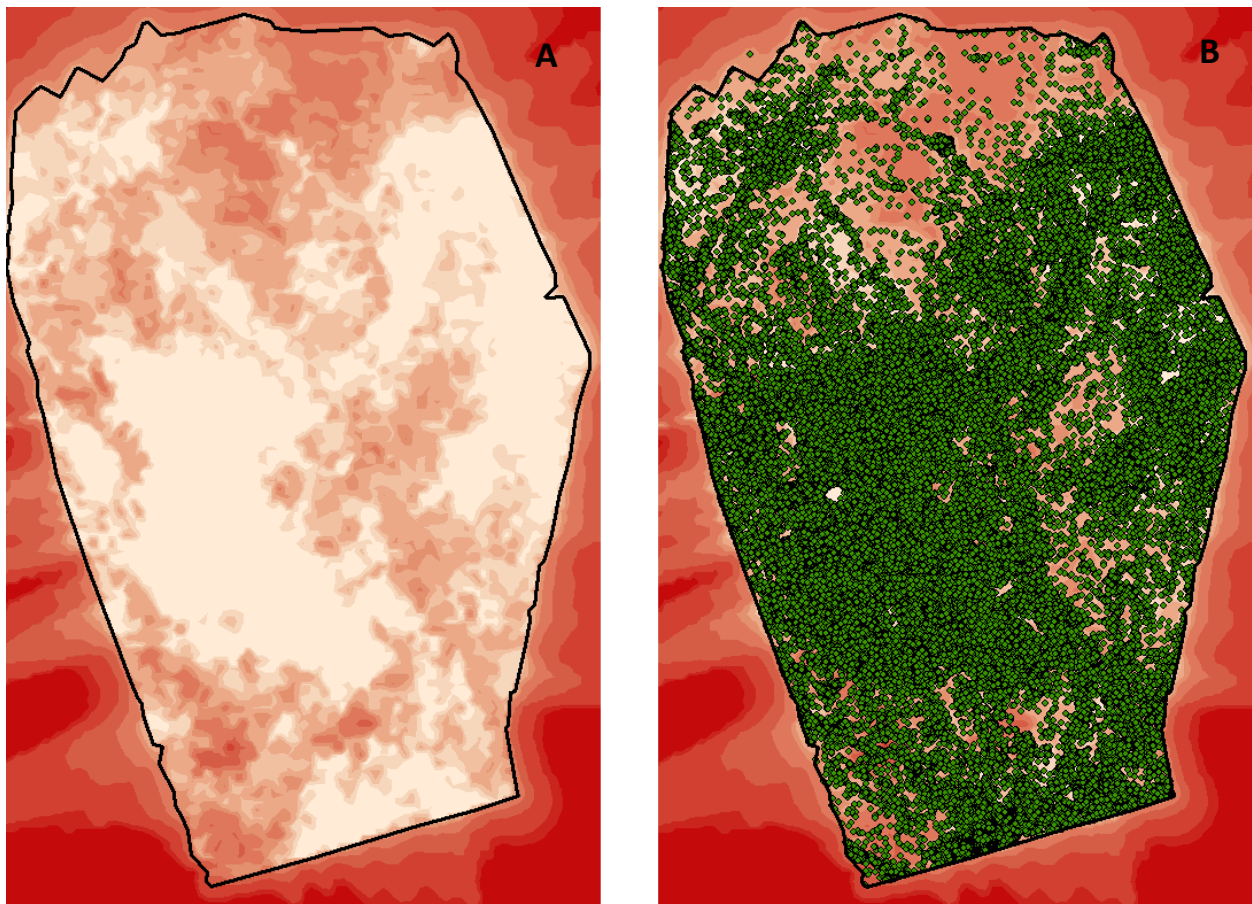


Figure 9: Prediction errors from EBK model.

parameters for the EBK tool, having a standardized RMS near one is a key factor in producing a reliable model. Once the standardized RMS has been accounted for, the model with the smallest RMS and ASE should be chosen (Krivoruchko and Krause, 2012).

### ***V.5.1 Standard Error Visualization***

Kriging tools can also create surfaces to visualize the predicted standard error, allowing the user to identify areas with low or high uncertainty. The standard error maps “may indicate if there are parts of a region where sampling should be increased to improve the estimates” (Fischer and Getis, 2010). The ability to assess the precision of the interpolation across the surface was a feature requested by the Permian Basin team. Standard error maps were generated for each of the parameters that were interpolated. Figure 10 shows an example of the standard error maps in an area of the Permian Basin. As demonstrated in Figure 10A, the lightly colored areas have a high degree of precision and low error rate, and the darker areas have more uncertainty associated with them. Just like with any interpolation model, where the control data is concentrated, the interpolation created the most accurate results. The control points used to create the error map are illustrated in Figure 10B with the data points overlaid on the prediction standard error map.



*Figure 10: Prediction standard error maps from EBK model without data points shown in Figure 10A and with control data shown in Figure 10B.*

## VI. RESULTS

### VI.1 CLASSIFYING WELLS BY HORIZONS

As mentioned in the challenges section of this report, a single formation can be more than 3,000 feet thick and contain multiple productive horizons. Figure 11 illustrates wells that are classified as producing from the same formation in the state's dataset.

Using the designations from the geologists, the wells were reclassified to the specific horizon within the formation they were producing from for further evaluation. Figure 12 shows the same set of wells as Figure 11, but the wells have been broken out and symbolized by the producing horizon.

This allowed the Permian Basin team to evaluate the reservoir properties and other attributes that are making a specific zone productive at a much more precise level than available with the state dataset. Figure 13 shows the wells from each horizon overlaid on the same map.

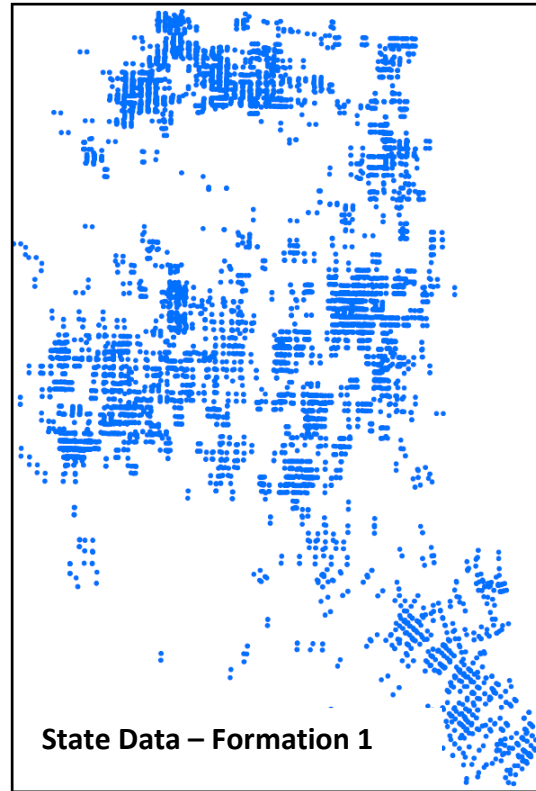


Figure 11: Blue points represent wells classified as producing from the same formation.

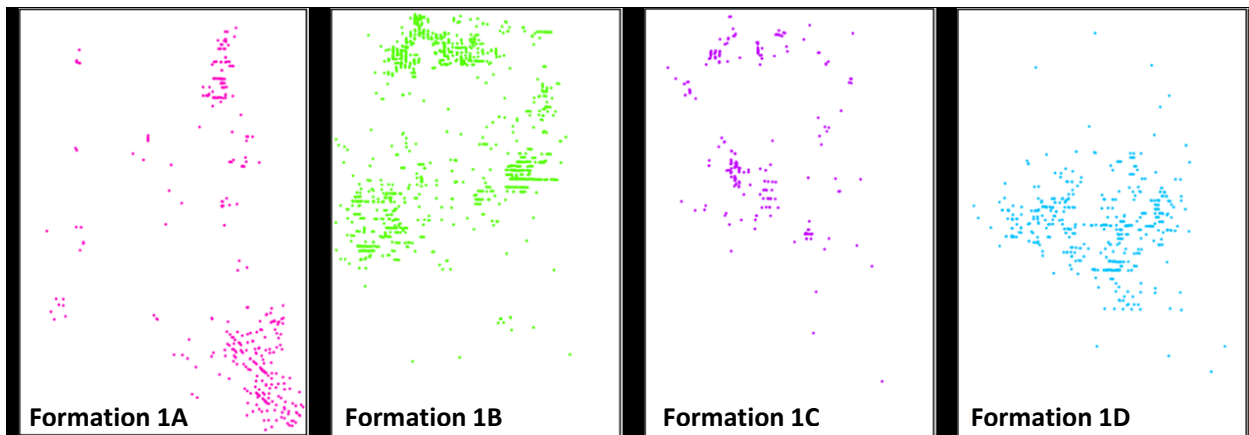
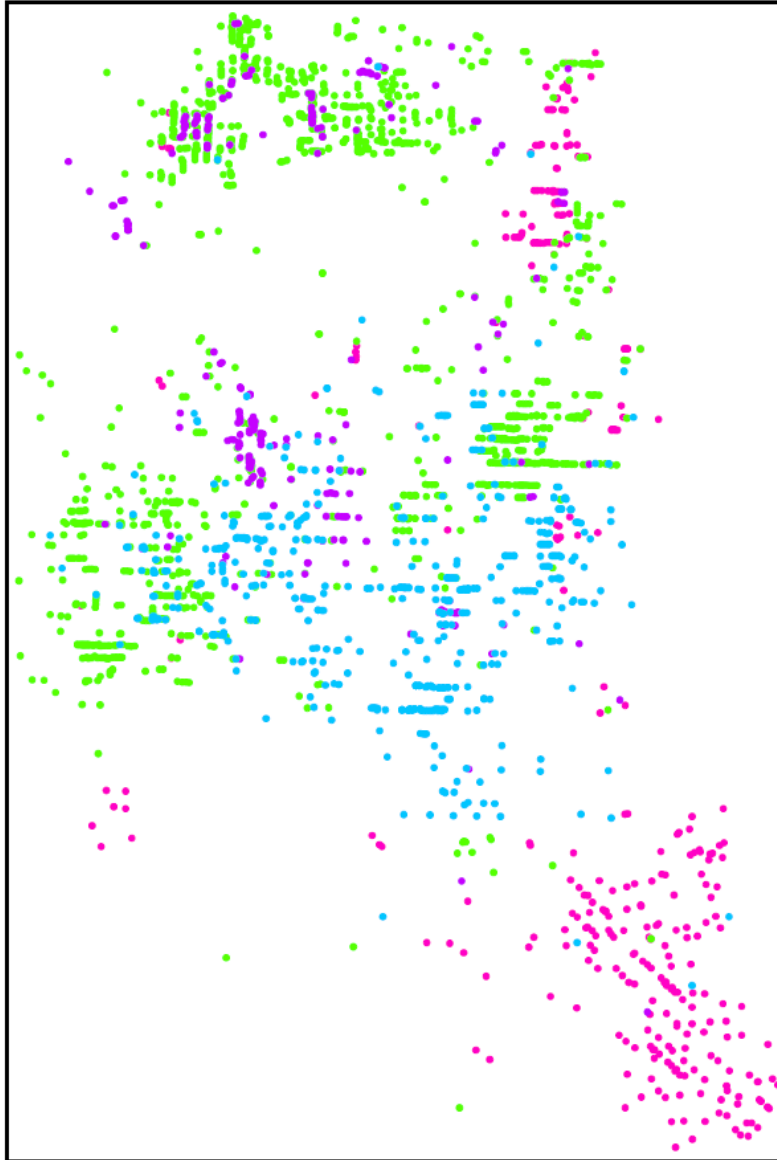


Figure 12: New well classifications from internal data applied to well dataset.



*Figure 13: Wells from each horizon in formation shown together.*

## **VI.2 INCORPORATING PETROPHYSICS**

The geologist assigns a petrophysical value to a well based on the average value of the property in the producing horizon at the well's location. The value of the curves can be indicative of reservoir characterizations (Boyce, 2015). The interpolated grids are used to provide a more holistic view of the horizon indicating which stacked characteristics provide the most potential production and assist with horizon valuation. Using the petrophysical metrics provided by the geologist, grids were created for gamma ray, resistivity, neutron porosity, and bulk density for each horizon. Values for these properties were extracted to the well bores for wells that were not interpreted by the geologists. This workflow is detailed in Figure 14.

Figure 14A shows well control points with internally interpreted petrophysical properties shown



symbolized from a low-to-high value. The geologist determined the value of the petrophysical property by taking an average value for the horizon. Next, Figure 14B depicts the creation of interpolated grids for each variable from the control points using the same EBK process.

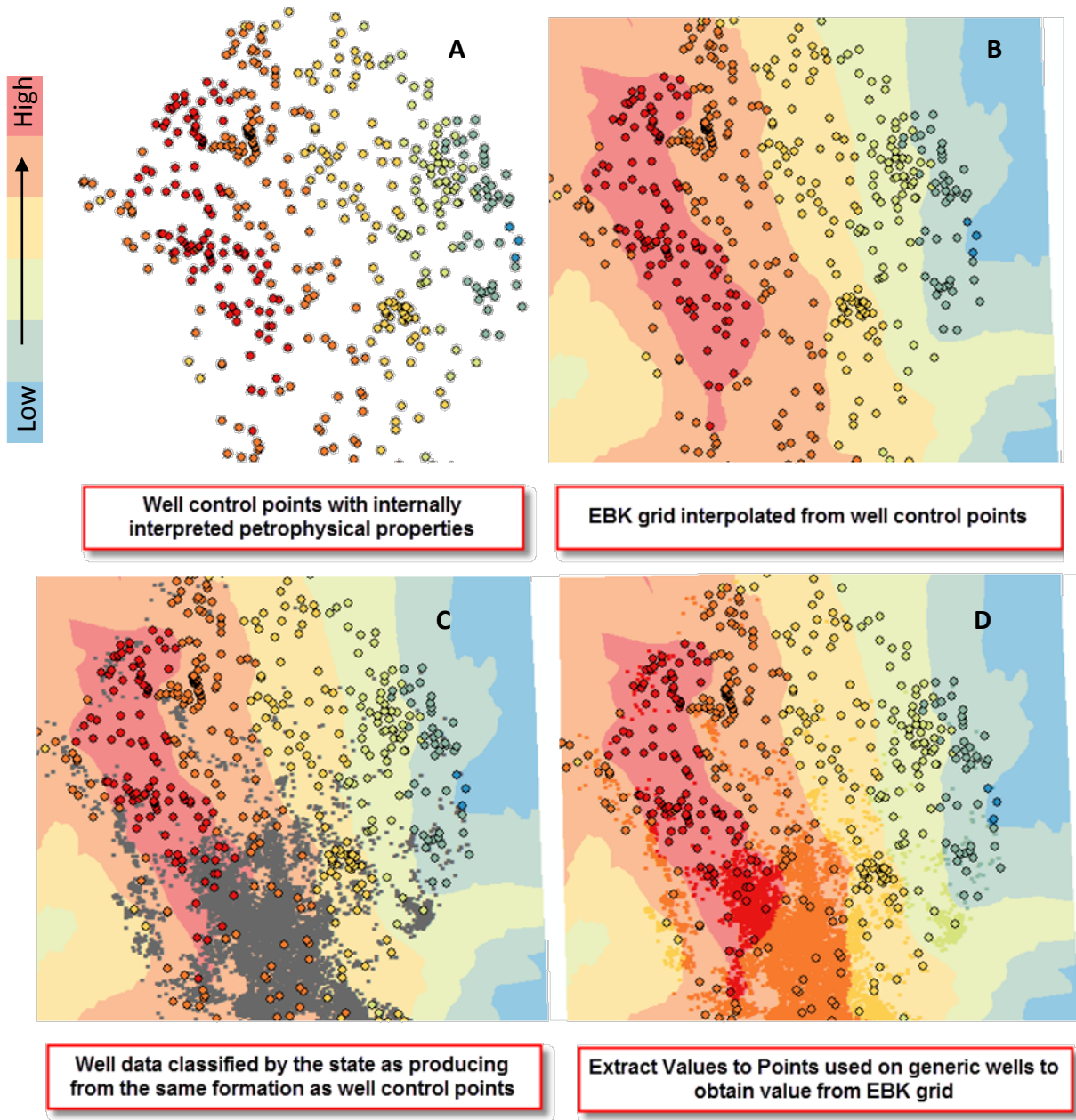


*Figure 14: Workflow for obtaining petrophysical values for wells that were not individually evaluated. This was achieved by extracting the value for each well from the EBK grid that models the petrophysical parameter.*

All wells that are classified as producing from the same formation in the state’s dataset that do not contain values for petrophysical properties are shown in grey on Figure 14C. Using the Extract Values to Points geoprocessing tool found in Esri’s Spatial Analysis toolbox, on the state’s well

dataset, the values for each of the petrophysical properties was extracted to the well bore based off the well's coordinate location. The well dataset from the state is shown symbolized by the new petrophysical value that was added to the well's attribute information in Figure 14D.

### VI.3 GENERATING 3D SURFACES

Once the well data was parsed out by horizon name, the geologist's SSTVD picks were utilized to generate interpolated surfaces across the basin for each geologic horizon using the EBK tool in GIS. Figure 15 illustrates the results of the EBK tool for one of the geologic horizons. Figure 15A is a 2D view of the horizon in GIS; Figure 15B is the same surface viewed in 3D perspective using Drilling Info's Transform software.

The output of the EBK tool is an ArcGIS geostatistical analyst (GA) layer. Instead of having a value at each well location, the GA layer provides a continuous surface. To use the surfaces in other programs and run further analyses on them, the GA layers were converted to raster grids using the GA Layer to Grid geoprocessing tool in ArcMap.

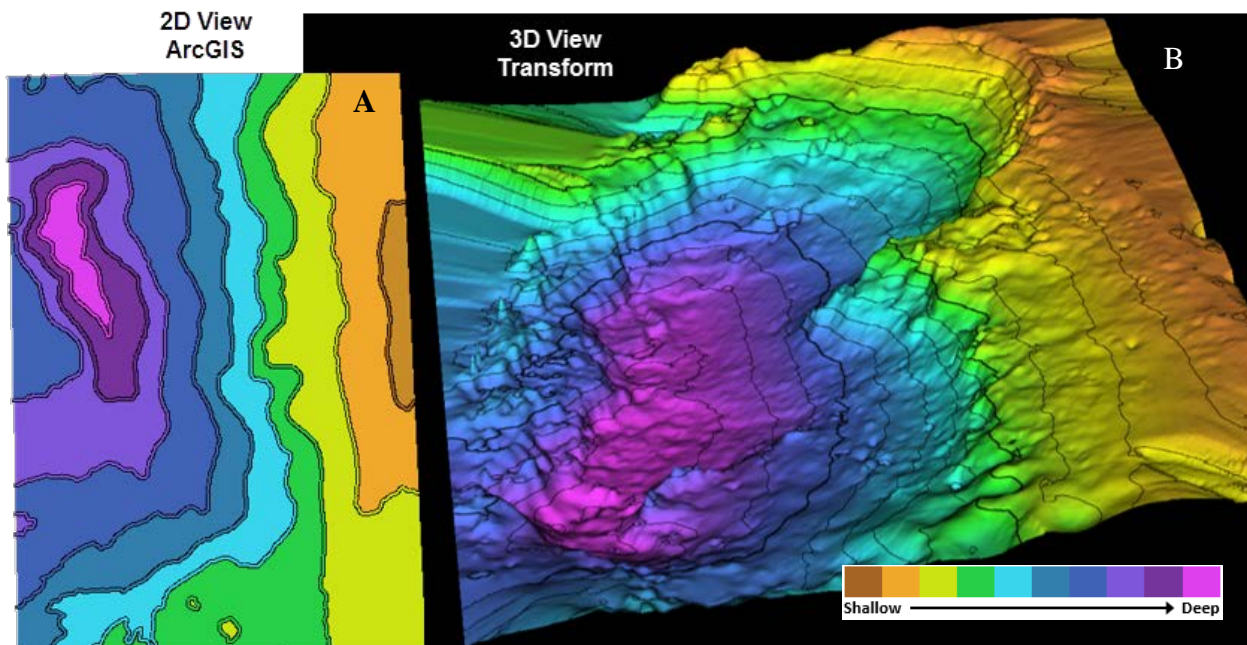


Figure 15: Screenshot of geologic horizon shown in 2D view in ArcMap (left) and in 3D view in Transform software (right). Horizon generated using EBK process in GIS. Transform screenshot provided by Cullen Hogan, Southwestern Energy, January 6, 2016.

### VI.4 VISUALIZING PRODUCTION

After the GA layers for the formation horizons and the petrophysical properties were converted to raster grids, they were supplied to the geophysicist for the basin team 3D model in Jewel Suite. This model provided a platform to visualize the integration of engineering and completions data extracted from well logs. The grids delineating the different horizons within the formations were used for a well landing zone analysis and reclassification of the producing formation that specified which

horizon the well produces from. Figure 16 depicts a snapshot of a cross-section from the 3D model using the interpolated geologic horizons with the well deviation surveys to identify where the wells are producing.

The model clearly shows multiple wells producing from stacked interval pay, and provides a different perspective than traditional 2D maps of the same wells. This added information creates a better understanding of how the basin works and which horizons are productive. By utilizing internally interpreted data instead of relying on the generic formation classifications from the state's regulatory information, the model provides a more precise assessment of activity in the Permian Basin.

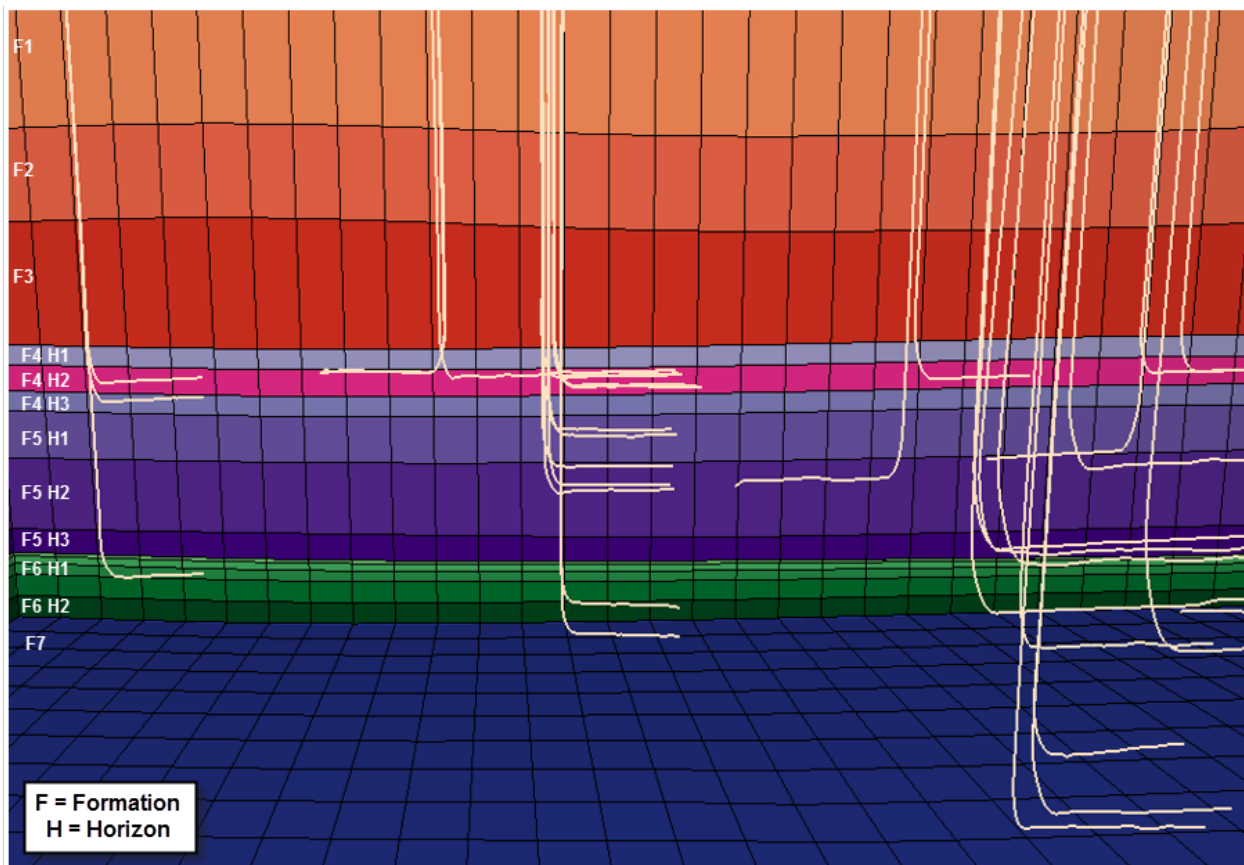


Figure 16: Screenshot of structural model in JewelSuite software displaying wells intersecting target formations. Screenshot provided by Cullen Hogan, Southwestern Energy, February 4, 2016.

## VII. SUMMARY

### VII.1 INTEGRATED PLATFORM

Figure 17 shows the challenge of working with the state well data. The distance between these zones is over 3,000 feet thick, yet all wells are shown classified as producing from a single formation in the state's dataset. GIS was used as a platform to interpolate grids from interpreted well log data. This methodology allowed the utilization of proprietary information to classify producing formations instead of relying on imprecise or unreliable state data.

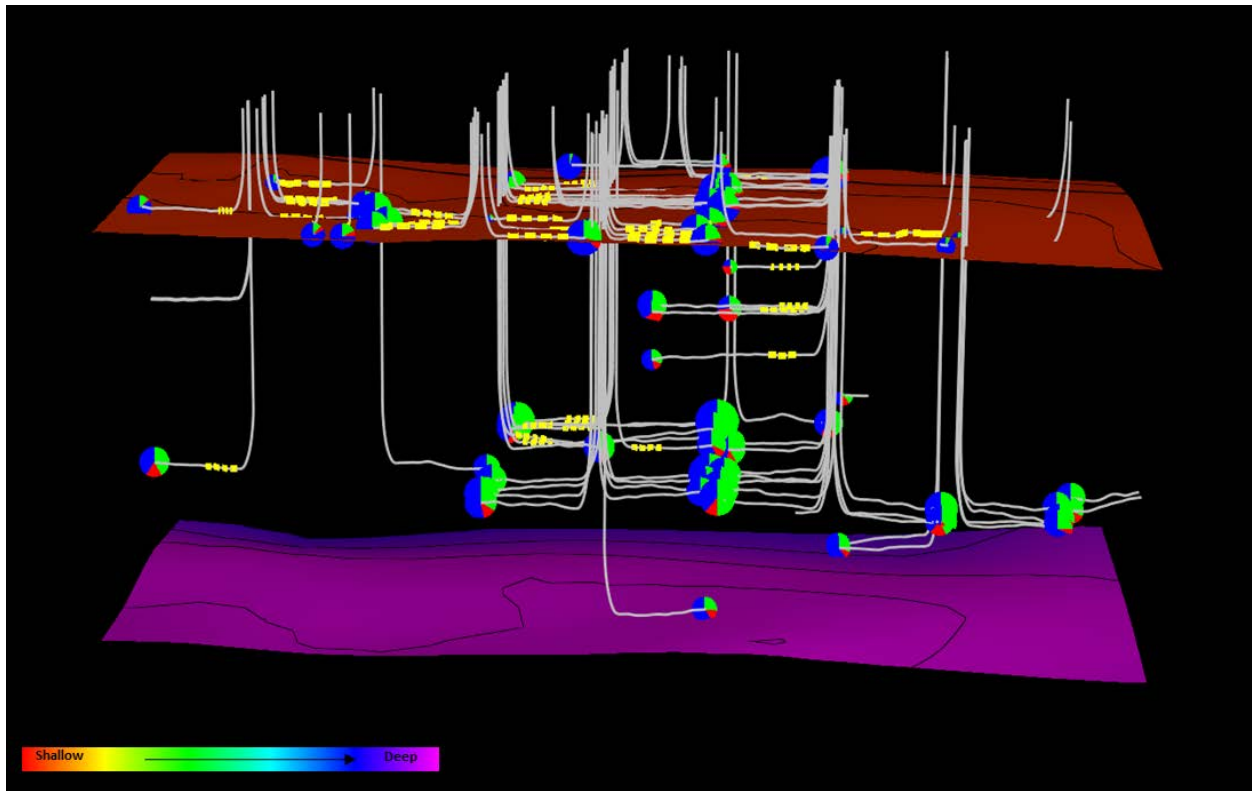


Figure 17: Image depicting surfaces of geologic horizons created in GIS using EBK, and depicted in 3D using Transform. The horizons are shown in conjunction with well deviation surveys; pie charts representing production, of oil (green), gas (red), and water (blue); and well completion stages displayed in yellow. The two surfaces are separated by more than 3,000 feet, but are classified in the State’s dataset as producing from the same formation. Screenshot provided by Cullen Hogan, Southwestern Energy, March 15, 2016.

This workflow provided a framework for streamlining assessment and systematically appraising basins. Values were extrapolated to areas without data so the team has a more complete picture of the basin. Examining the data in an integrated environment allowed for classification of trends that may otherwise have been unidentified (Figure 18). Evaluation of the producing horizons, in addition to the geologic, petrophysical, and engineering properties helped identify trends related to petroleum production and increased the team’s understanding of the relationship between variables that allow for a play to be successful. It has created value by providing a faster learning curve for the team, rendering higher confidence levels, and delivering a better understanding of reservoir heterogeneity.

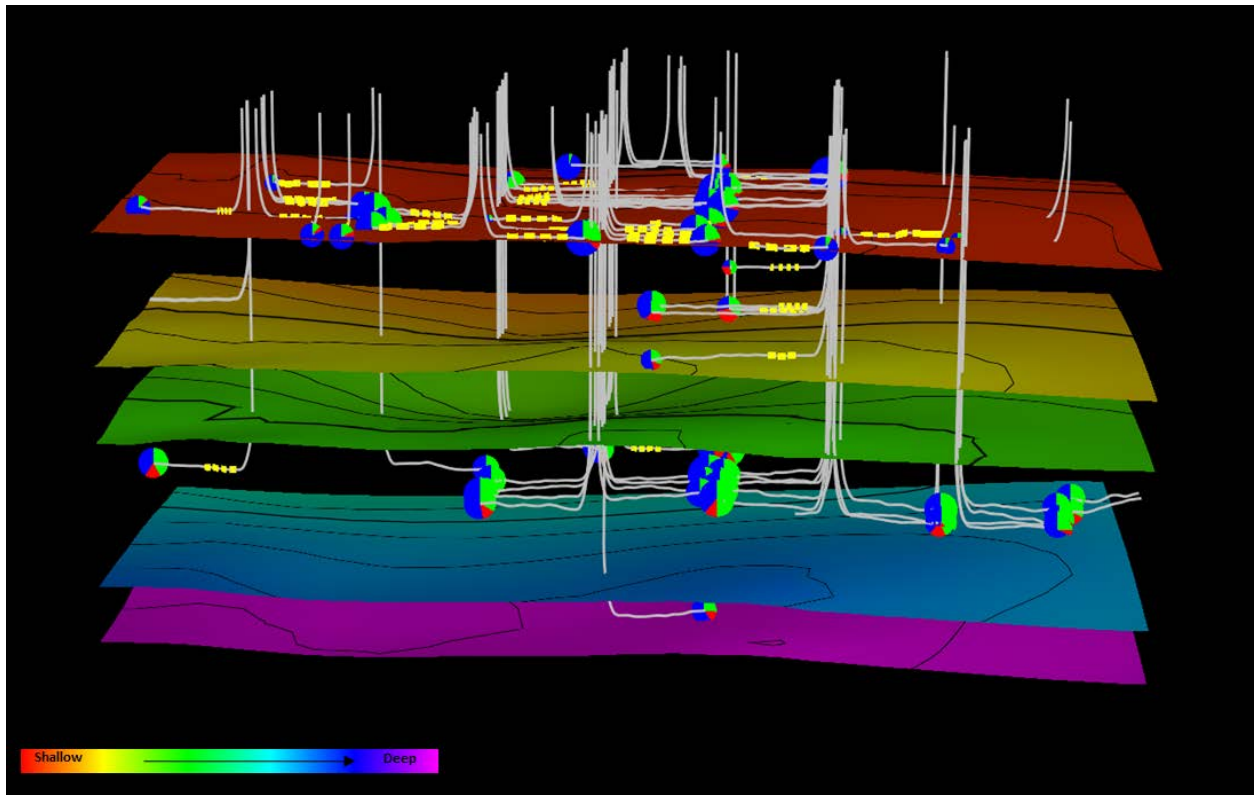


Figure 18: Image depicting a formation sub-delineated into multiple geologic horizons, and depicted in 3D using Transform. Screenshot provided by Cullen Hogan, Southwestern Energy. March 15, 2016.

## ACKNOWLEDGEMENTS

I would like to thank Southwestern Energy's Permian Basin team, specifically Cullen Hogan and Matt Boyce for their technical expertise and guidance on basin evaluation, Jeremy Andrews from Southwestern Energy for his helpful suggestions and editing comments, and my Penn State University advisor, Dr. Patrick Kennelly for his direction throughout the project.

## REFERENCES

- Achilleos, Georgios. "Errors within the Inverse Distance Weighted (IDW) Interpolation Procedure." *TGEI Geocarto Int. Geocarto International* 23.6 (2008): 429-449. Print.
- Asquith, George B. and Daniel Krygowski. *Basic Well Log Analysis*. Tulsa, OK: American Association of Petroleum Geologists, 2004. Print.
- Boyce, Matt. Interpreted well log. Digital image. Southwestern Energy, 2013. 7 Dec. 2015.
- Boyce, Matt. Personal interview. Southwestern Energy, 2015. 7 Dec. 2015.
- Castruccio, Stefano, Luca Bonaventura, and Laura M. Sangalli. "A Bayesian Approach to Spatial Prediction With Flexible Variogram Models." *Journal of Agricultural, Biological, and Environmental Statistics JABES* 17.2 (2012): 209-27. Print.
- Chen, Chuanfa, Na Zhao, Tianxiang Yue, and Jinyun Guo. "A Generalization of Inverse Distance Weighting Method via Kernel Regression and Its Application to Surface Modeling." *Arabian Journal of Geosciences Arab J Geosci* 8.9 (2014): 6623-633. Print.
- Chiles, Jean-Paul, and Pierre Delfiner. *Geostatistics: Modeling Spatial Uncertainty*. Hoboken, NJ: Wiley, 2012. Print.
- Curth, Patrick J., James R. Courtier, Gary B. Smallwood, Rick Mauro, and Scot Evans. "Earth Model Assists Permian Asset Valuation." *Oil & Gas Journal* 113.7 (2015). Print.
- Dynamic Graphics. "4D Quantitative Analysis." *CoViz 4D Software*. 2015. Web. 10 Dec. 2015.
- Esri. "Exploratory Spatial Data Analysis (ESDA)." *Geostatistical Analyst*. Web. 9 Jan. 2016.
- Esri. "Evaluating Interpolation Results." *Geostatistical Analyst*. Web. 9 Jan. 2016.
- Esri. "What Is Empirical Bayesian Kriging?" Web. 10 Dec. 2015.
- Fischer, Manfred M., and Arthur Getis. *Handbook of Applied Spatial Analysis: Software Tools, Methods and Applications*. Berlin: Springer, 2010. Print.
- Flitter, Helmut, Phillip Weckenbrock, Robert Weibel, and Samuel Wiesmann. Geographic Information Technology Training Alliance (GITTA). "Continuous Spatial Variables." Vers. 24.10.2013. Web. 10 Jan. 2016.
- Hogan, Cullen. Screenshot from *JewelSuite Subsurface Modeling 2014.2*. Computer software. Vers. 5.1.68.0. Halliburton. 4 Feb. 2016.

- Hogan, Cullen. Screenshot from *Transform*. Computer software. Drilling Info. 6 Jan. 2016.
- Johnston, Kevin, Jay M. Ver Hoef, Konstantin Krivoruchko, and Neil Lucas. "Using ArcGIS Geostatistical Analyst." Esri, 2001. Web. 10 Jan. 2016.
- Krivoruchko, Konstantin. "Empirical Bayesian Kriging Implemented in ArcGIS Geostatistical Analyst." ArcUser Fall 2012 Ed. (2012). Print.
- Krivoruchko, Konstantin, and Eric Krause. "Concepts and Applications of Kriging." Esri, 24 July 2012. Web. 10 Jan. 2016.
- Lampiris, Nikolaos. "Introduction to ESRI Geostatistical Analyst Using Interpolation Tools." *GIS-box*. 14 Oct. 2015. Web. 6 Jan. 2016.
- Matador Resources Company. "Investor Presentation." Securities Exchange Commission Form 8-K, Exhibit 99.1. 10 May. 2015. Web. 5 Nov. 2015.
- Murchison Oil & Gas. "Geographic Footprint." 2010. Web. 9 Oct. 2015.
- "NIST/SEMATECH e-Handbook of Statistical Methods." Apr. 2012. Web. 15 Feb. 2016.
- Olea, Ricardo A. *Geostatistics for Engineers and Earth Scientists*. Kansas Geological Survey. Springer, 2013. Print.
- O'Sullivan, David, and David J. Unwin. *Geographic Information Analysis*. 2nd ed. Hoboken, NJ: John Wiley & Sons, 2010. Print.
- Pardo-Igúzquiza, Eulogio, and Peter A. Dowd. "Empirical Maximum Likelihood Kriging: The General Case." *Mathematical Geology Math Geol* 37.5 (2005): 477-92. Print. Shale Experts. "Permian Basin Overview." 2015. Web. 13 Nov. 2015.
- Pilz, Jürgen, and Gunter Spöck. "Why Do We Need and How Should We Implement Bayesian Kriging Methods." *Stochastic Environmental Research and Risk Assessment Stoch Environ Res Risk Assess* 22.5 (2007): 621-32. Print.
- Shi, Wenzhong, Anthony G. O. Yeh, Yee Leung, and Chenghu Zhou, eds. *Advances in Spatial Data Handling and GIS: 14th International Symposium on Spatial Data Handling*. New York: Springer Verlag, 2012. Print.